Structural Correlation and Metal Ion Movement in Stable Pentaammineruthenium(III)–Hypoxanthine Complexes

M. E. Kastner, K. F. Coffey, M. J. Clarke,* S. E. Edmonds, and K. Eriks

Contribution from the Departments of Chemistry, Boston College, Chestnut Hill, Massachusetts 02167, and Boston University, Boston, Massachusetts 02215.
Received January 26, 1981. Revised Manuscript Received April 30, 1981

Abstract: The crystal and molecular structures of 7-[(Hyp)$(NH_3)_5$Ru]$Cl_3 \cdot 3H_2O$ and 9-[(7-MeHyp)$(NH_3)_5$Ru]Cl_3 are reported. Crystals of both compounds belong to the orthorhombic space group *Pnma* with unit cell dimensions: a = 11.465 (3) Å, b = 6.820 (2) Å, and c = 22.520 (9) Å for the former; a = 11.146 (4) Å, b = 6.835 (2) Å, and c = 21.490 (9) Å for the latter. The hypoxanthine complex was prepared under neutral to mildly acidic conditions with deoxyinosine as the initial ligand. Chromatographic analysis of the final product showed the 7-coordinated complex to be the only monomeric species present, which verifies N(7) as the preferred coordination site for $(NH_3)_5Ru^{II,III}$ ions with inosine and guanosine ligands. When hypoxanthine or 7-methylhypoxanthine were employed as ligand, the 3- and 9-coordinated isomers formed. Under acidic conditions the $(NH_3)_5Ru^{III}$ was observed to undergo linkage isomerization from the N(3) to the N(9) positions with a rate of 1.25×10^{-4} s^{-1} at 37 °C, whereas in neutral media this rate was depressed to 2.2×10^{-6} s^{-1}, due to proton ionization from the N(1) site. Activation parameters in acidic media are $\Delta H^{\ddagger}$ = 90 kJ/mol and $\Delta S^{\ddagger}$ = −31 J/(mol K). An empirical correlation is found between ΔpK_a values of various ruthenium(III)–purine, –pyrimidine, and –imidazole complexes and $1/r^2$, where r is the distance between the metal ion and the deprotonation site. A similar correlation is observed between $1/r^2$ and the decrease in the Ru(III) reduction potential, ΔE, on deprotonation of the complexes. A free energy correlation is also noted between the ΔpK_a and ΔE values for these complexes.

The coordination of transition-metal ions to nucleotides, nucleic acids, and their constituent bases has assumed an increasing importance in recent years due to the mutagenicity[1] and anticancer activity of a number of transition-metal complexes.[2-4] In particular, recent studies have shown that a range of ruthenium complexes are mutagenic[5-7] and several also show promise in the development of anticancer pharmaceuticals.[8,9]

The pentaammineruthenium(III)–hypoxanthine compounds treated here were initially prepared in an effort to establish the differing physical and chemical effects of a metal ion firmly coordinated at various sites on a purine ring. The effects of varying the coordination site between the N(3), N(7), and N(9) positions on (1) the ligand to metal charge-transfer bands, (2) the acidity of the ligand, and (3) the reduction potential of the metal ion have since been reported.[10] In order to assign the various linkage isomers unequivocally, it was also necessary to firmly establish the molecular structures of at least two of the three possible isomers. Moreover, since deoxyinosine, which was employed in the synthesis of the N(7)-coordinated hypoxanthine complex, provides an excellent model for guanosine ligands, the structure determination of this complex coupled with a correspondence in spectroscopic and chemical properties makes it possible to verify the coordination site of pentaammineruthenium(III) on various guanosine ligands and on these ligands in nucleic acids.

In previous investigations it had been shown that the N(3)-bound isomer undergoes linkage isomerization to the N(9)-coordinated form in acidic media.[10] The work reported here quantitates the rate of this isomerization and further shows that the same process occurs (with a significantly dimiminished rate) even at neutral pH.

Finally, the structural parameters made available from this and other studies of pentaammineruthenium(III) complexes with purine, pyrimidine, and imidazole ligands provide the basis for several empirical linear free energy correlations. These relationships allow the prediction of the acidic properties of the ligand and the reduction potential of the metal or can be used to estimate the distance between the metal coordination and proton ionization sites in new complexes.

Experimental Section

Chemicals and Reagents. The hypoxanthine complexes were prepared by previously reported methods.[10] All kinetic runs were done at an ionic strength adjusted to 1.0 with a standard LiCl solution and with buffer concentrations in the range of 0.17–0.2 M. Buffers employed in the appropriate pH ranges were HCl, pH 0–1.85, glycine/HCl, pH 2–3.7, sodium acetate/acetic acid, pH 4–5, and phosphate, pH 5–7.

Kinetic Studies. Kinetic studies were performed spectrophotometrically or by using an HPLC technique to follow the concentrations of the reactants or products. Spectrophotometric results were obtained on a Perkin-Elmer Model 575 spectrophotometer with temperature control of the cuvette compartment held within ±0.1 °C. The change in absorbance was followed at 325 nm over at least 6 half-lives, and the data over the first 2–3 half-lives were treated by the method of Guggenheim[13] as a first-order reaction and then fitted by a standard nonweighted linear least-squares method to determine the observed rate. Above pH 5.2 isosbestic points were no longer observed over the entire course of the reaction and HPLC was used to monitor reactant and product concentrations.

Product analysis by HPLC was performed by injecting samples onto a Varian Model 5000 HPLC fitted with a Varian CH-10 or a Waters Micro-Bondapak-C-18 column and a Varichrome UV–visible detector. A 0.2 M solution of ammonium propionate at pH 5.5 was used as the eluant. Capacity factors for the N(3) and N(9) isomers under these conditions were 1.9 and 1.7, respectively. Concentrations were followed by peak-height analysis.

Rate constants were obtained from a weighted least-squares fit of eq 1 to a plot of k_{obsd} vs. $[H^+]$.[13] Values of $\Delta H^{\ddagger}$ and $\Delta S^{\ddagger}$ were obtained from a linear regression analysis of a plot of ln (k_1/T) vs. $1/T$.

Crystallography. Single crystals of 7-[(Hyp)$(NH_3)_5$Ru]$Cl_3 \cdot 3H_2O$ and 9-[(7-MeHyp)$(NH_3)_5$Ru]Cl_3 were grown by ethanol diffusion into 0.1 M HCl solutions of the respective complexes. An orange single crystal

* Address correspondence to this author at Boston College.

(1) Flessel, C. P. In "Trace Metals in Health and Disease"; Kharasch, N., Ed.; Raven Press: New York, 1980; pp 109–122 and other articles in this volume.
(2) Barton, J. K.; Lippard, S. J. *Met. Ions Biol.* **1980**, *1*, 31–114.
(3) Marzilli, L. G.; Kistenmacher, T. J.; Eichhorn, G. L. *Met. Ions Biol.* **1980**, *1*, 179–250.
(4) See various articles in *Met. Ions Biol. Syst.* **1980**, **10** and **11**.
(5) Yasbin, R. E.; Matthews, C. R.; Clarke, M. J. *Chem.-Biol. Interact.* **1980**, *31*, 355–365.
(6) Clarke, M. J. *Inorg. Chem.* **1980**, *19*, 1103–1104.
(7) Durig, J. R.; Danneman, J.; Behnke, W. D.; Mercer, E. E. *Chem.-Biol. Interact.* **1976**, *13*, 287.
(8) Clarke, M. J. In "Inorganic Chemistry in Biology and Medicine"; Martell, A. E., Ed.; American Chemical Society: Washington, DC, 1980; in press.
(9) Clarke, M. J. *Met. Ions Biol. Syst.* **1980**, *11*, 231–283.
(10) Clarke, M. J. *Inorg. Chem.* **1977**, *16*, 738.
(11) Clarke, M. J.; Taube, H. *J. Am. Chem. Soc.* **1975**, *97*, 1397.
(12) Clarke, M. J. *J. Am. Chem. Soc.* **1978**, *100*, 5068–5075.
(13) Wilkins, R. G. "The Study of Kinetics and Mechanism of Reactions of Transition Metal Complexes"; Allyn and Bacon: Boston, 1974; pp 13–45.

0002-7863/81/1503-5747$01.25/0

Table I. Atomic Coordinates[a] in the Unit Cell

	N(7)-[(Hyp)$(NH_3)_5$Ru]$Cl_3 \cdot 3H_2O$			N(9)-[(7-MeHyp)$(NH_3)_5$Ru]Cl_3		
atom	x	y	z	x	y	z
Ru	0.1261 (1)	1/4	0.1458 (1)	0.1822 (1)	1/4	0.1463 (1)
Cl(1)	0.8739 (3)	1/4	−0.0043 (1)	0.3247 (2)	1/4	0.3196 (1)
Cl(2)	0.7570 (2)	1/4	0.1761 (1)	0.3907 (2)	1/4	0.4961 (1)
Cl(3)	−0.0018 (4)	3/4	0.2328 (2)	0.4315 (2)	1/4	0.7396 (1)
N(1)	0.5518 (7)	1/4	0.0805 (5)	0.6147 (6)	1/4	0.0133 (3)
C(2)	0.5701 (9)	1/4	0.0219 (5)	0.5863 (7)	1/4	0.0747 (4)
N(3)	0.4898 (9)	1/4	−0.0179 (4)	0.4769 (6)	1/4	0.0962 (3)
C(4)	0.3815 (10)	1/4	0.0056 (4)	0.3928 (6)	1/4	0.0503 (4)
C(5)	0.3515 (8)	1/4	0.0657 (5)	0.4153 (7)	1/4	−0.0122 (3)
C(6)	0.4419 (9)	1/4	0.1080 (5)	0.5361 (7)	1/4	−0.0355 (4)
N(7)	0.2320 (7)	1/4	0.0704 (4)	0.3041 (6)	1/4	−0.0412 (3)
C(8)	0.1920 (9)	1/4	0.0148 (5)	0.2205 (7)	1/4	0.0039 (3)
N(9)	0.2793 (8)	1/4	−0.0250 (4)	0.2712 (5)	1/4	0.0605 (3)
N(10)	0.2258 (6)	0.4708 (11)	0.1868 (3)	0.0610 (4)	0.0336 (7)	0.1162 (3)
N(11)	0.0171 (5)	0.4681 (10)	0.1087 (3)	0.2964 (4)	0.0292 (7)	0.1815 (2)
N(12)	0.0228 (8)	1/4	0.2217 (4)	0.0939 (5)	1/4	0.2325 (3)
C(13)				0.2790 (8)	1/4	−0.1087 (4)
O(1)	0.4346 (7)	1/4	0.1622 (3)	0.5689 (5)	1/4	−0.0904 (3)
O(2)	0.2434 (11)	0.6984 (21)	0.3544 (6)			
O(3)	0.6024 (7)	1/4	−0.1331 (3)			

[a] The numbers in parentheses are the estimated standard deviations in the last significant figure.

Table II. Bond Lengths (Å) in Pentaammineruthenium-Hypoxanthine Complexes[a]

	bond lengths			bond lengths	
type	N(7)-[Hyp]	N(9)-[7-MeHyp]	type	N(7)-[Hyp]	N(9)-[7-MeHyp]
Ru–N(7)	2.087 (9)		C(4)–C(5)	1.397 (14)	1.366 (10)
Ru–N(9)		2.094 (6)	C(4)–N(9)	1.360 (14)	1.373 (9)
Ru–N(10)	2.105 (7)	2.105 (4)	C(5)–C(6)	1.407 (15)	1.436 (11)
Ru–N(11)	2.115 (7)	2.115 (4)	C(5)–N(7)	1.375 (13)	1.387 (10)
Ru–N(12)	2.081 (9)	2.097 (6)	C(6)–O(1)	1.224 (13)	1.234 (10)
N(1)–C(2)	1.337 (16)	1.357 (10)	N(7)–C(8)	1.334 (14)	1.343 (9)
N(1)–C(6)	1.403 (14)	1.366 (10)	N(7)–C(13)		1.477 (9)
C(2)–N(3)	1.285 (15)	1.305 (10)	C(8)–N(9)	1.344 (14)	1.342 (9)
N(3)–C(4)	1.350 (15)	1.362 (10)			

[a] The number in parentheses is the estimated standard deviation in the last significant figure.

of the N(7) compound with approximate dimensions 0.24 × 0.30 × 0.35 mm and a yellow single crystal of the N(9) compound with approximate dimensions 0.38 × 0.22 × 0.24 mm were used for X-ray diffraction studies. Both compounds were found to crystallize in the orthorhombic space group *Pnma* with unit cell dimensions: a = 11.465 (3) Å, b = 6.820 (2) Å, and c = 22.520 (9) Å for the former; a = 11.146 (4) Å, b = 6.835 (2) Å, and c = 21.490 (9) Å for the latter. Unit cell dimensions were determined by least-squares refinement of 15 reflections having $2\theta \geq 20°$ as centered on a Syntex $P2_1$, four-circle diffractometer. With Z = 4 and molecular formulations of $H_{25}C_5N_9O_4Cl_3Ru$ and $H_{21}C_6N_9OCl_3Ru$, calculated (experimental) densities are 1.81 (1.75) g/cm^3 and 1.79 (1.80) g/cm^3. Experimental densities were determined by flotation in mixtures of CCl_4 and $HCBr_3$.

Diffraction data were collected by using the θ–2θ scanning technique and graphite-monochromated Mo Kα radiation (λ = 0.71069 Å). Scan rates of 2.0–10.0°/min were employed. Background was collected for 0.5 times the time of the scan with a scan range of 0.7° below Kα_1 and above Kα_2. Crystal stability was monitored by measuring four standard reflections every 50 reflections. No significant variation in the intensity of the standards was observed. All independent data having $(\sin\theta)/\lambda = 0.649$ Å^{-1} ($\theta \leq 27.5°$) for the N(7)-coordinated compound and $(\sin\theta)/\lambda = 0.595$ Å^{-1} ($\theta \leq 25°$) for the N(9)-bound isomer were collected. No absorption corrections were applied (linear absorption coefficients were 13.5 and 14.5 cm^{-1} for the two crystals, respectively).

Data reduction, solution, and refinement of the structures were accomplished by using the XRAY-76 Crystallographic Computer Program System.[14] The Patterson function was used to locate the Ru atoms, and all nonhydrogen atoms were located in subsequent difference Fourier maps. Full-martix least-squares refinement of 1260 and 1255 observed reflections ($F_o \geq 3\sigma(F_o)$) with use of $1/\sigma^2(F_o)$ weighting was employed for the two crystals, respectively. Electron density maxima corresponding to most of the hydrogen atoms appeared in the difference maps. All hydrogen atoms were idealized with X–H distances of 0.95 Å on tetrahedral ammines and on bisectors of the hypoxanthine ligand. All hydrogens were given a fixed isotropic temperature factor (B = 4.0 Å^2).

In the final model for the N(7)-coordinated complex one oxygen atom of a water molecule, O(2), was taken as isotropic and assigned half-occupancy with disorder across the mirror plane. All other nonhydrogen atoms were anisotropic. In the final model for the N(9)-bound complex all nonhydrogen atoms were assigned anisotropic thermal motion.

Data to parameter ratios for the N(7)- and N(9)-coordinated complexes, respectively, are 10.6 and 10.9 with final unweighted R values ($R = \sum||F_o| - |F_c||/\sum|F_o|$) of 0.050 and 0.034. Atomic scattering factors for the nonhydrogen atoms were taken from Cromer and Mann[15] and those for hydrogen atoms from Stewart.[16]

Distances between the ruthenium and the various purine nitrogens were calculated directly from the data reported here for the N(7)- and N(9)-coordinated hypoxanthine complexes. In the case of other purine ligands these distances were calculated by using the geometries around the metal ion reported here for the N(7)- and N(9)-coordinated isomers, respectively, and crystallographic data for the ligand in question. The latter included hypoxanthine,[17] 7-methylxanthine,[18] guanine,[19] theophylline,[20] and imidazole.[21] The data of Graves and Hodgson[22] were

(14) Stewart, J. M. Technical Report TR-446 of the Computer Science Center; University of Maryland: College Park, MD.

(15) Cromer, C.; Mann, J. *Acta Crystallogr., Sect. A* **1968**, *A24*, 321.

(16) Stewart, R. F.; Davidson, E.; Simpson, W. *J. Chem. Phys.* **1968**, *42*, 3175.

(17) Values for r in the N(3)-coordinated hypoxanthine complexes were calculated by assuming a Ru–N bond distance of 2.11 Å and the geometry reported here for the hypoxanthine ligand.

(18) Kistenmacher, J.; Sorrell, T. *Acta Crystallogr., Sect. B* **1975**, *B31*, 489–492.

(19) Thewalt, U.; Bugg, C. E.; Marsh, R. E. *Acta Crystallogr., Sect. B* **1971**, *B27*, 2358.

(20) Sutor, D. J. *Acta Crystallogr.* **1958**, *11*, 83–87.

(21) Will, G. *Z. Kristallogr., Kristallgeom., Kristallphys., Kristallchem.* **1969**, *129*, 211.

(22) Graves, B. J.; Hodgson, D. J. *J. Am. Chem. Soc.* **1979**, *101*, 5608.

Table III. Bond Angles (Deg) in Pentaammineruthenium-Hypoxanthine Complexes[a]

type	bond angles		type	bond angles	
	N(7)-[Hyp]	N(9)-[7-MeHyp]		N(7)-[Hyp]	N(9)-[7-MeHyp]
N(7)RuN(10)	92.3 (2)		C(2)N(3)C(4)	112.7 (9)	112.7 (6)
N(7)RuN(11)	91.3 (2)		N(3)C(4)C(5)	127.3 (10)	125.9 (7)
N(7)RuN(12)	179.1 (8)		N(3)C(4)N(9)	126.5 (9)	124.3 (7)
N(9)RuN(10)		91.9 (2)	C(5)C(4)N(9)	106.2 (9)	109.8 (6)
N(9)RuN(11)		91.7 (2)	C(4)C(5)C(6)	118.3 (9)	121.0 (7)
N(9)RuN(12)		179.7 (18)	C(4)C(5)N(7)	108.7 (9)	106.1 (6)
N(10)RuN(11)	89.5 (3)	89.7 (2)	C(6)C(5)N(7)	133.0 (10)	133.0 (7)
N(10)RuN(12)	87.1 (2)	88.3 (2)	N(1)C(6)C(5)	111.3 (9)	109.5 (7)
N(11)RuN(12)	89.3 (2)	88.1 (2)	N(1)C(6)O(1)	120.1 (10)	122.8 (7)
RuN(7)C(8)	124.4 (7)		C(5)C(6)O(1)	128.7 (10)	127.6 (7)
RuN(7)C(5)	130.0 (7)		C(5)N(7)C(8)	105.6 (8)	107.3 (6)
RuN(9)C(8)		126.8 (5)	C(5)N(7)C(13)		127.5 (6)
RuN(9)C(4)		127.5 (5)	C(8)N(7)C(13)		125.2 (6)
C(2)N(1)C(6)	125.2 (9)	126.7 (7)	N(7)C(8)N(9)	111.8 (9)	111.2 (6)
N(1)C(2)N(3)	125.1 (10)	124.3 (7)	C(4)N(9)C(8)	107.7 (8)	105.7 (6)

[a] The number in parentheses is the estimated standard deviation in the last significant figure.

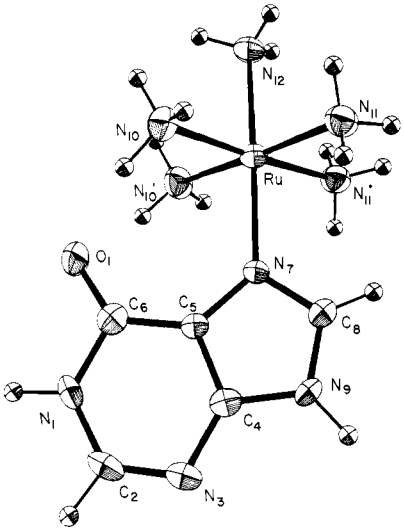

Figure 1. ORTEP[7] drawn model in perspective of 7-[(Hyp)$(NH_3)_5Ru]^{3+}$. Each atom is represented by an ellipsoid having an orientation and relative size analogous with the thermal parameters for each atom. The thermal ellipsoids are contoured at the 50% probability level.

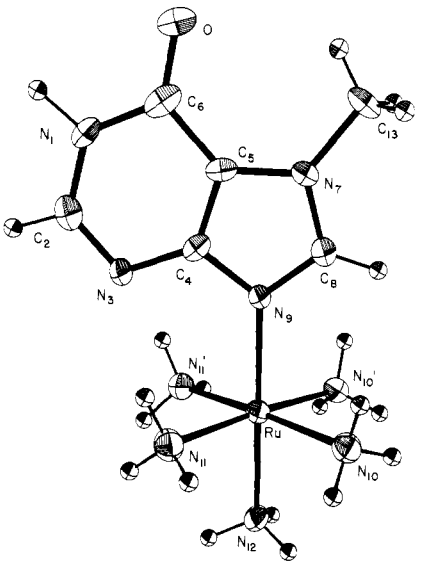

Figure 2. ORTEP[7] model of 9-[(7-MeHyp)$(NH_3)_5Ru]^{3+}$, prepared as in Figure 1.

employed in the calculation of ruthenium to nitrogen distances when the metal is coordinated to the exocyclic nitrogen on cytosine and adenine derivatives.

Results

Description of Structures. The structures of 7-[(Hyp)-$(NH_3)_5Ru]^{3+}$ and 9-[(7-MeHyp)$(NH_3)_5Ru]^{3+}$ are shown in Figures 1 and 2, respectively. The atomic coordinates for the crystallographically unique atoms are given in Table I. Thermal parameters associated with each atom are given as supplementary material on microfilm. Bond distances and bond angles for each complex are given in Tables II and III.

The coordination sphere around the ruthenium in each complex is essentially octahedral with Ru–NH_3 bond distances quite similar to those observed in other ammineruthenium(III) compounds.[22,23] While the Ru–N bond distances to the purine nitrogen and to the ammonia group trans to the purine ligand are perhaps slightly shorter than those to the cis ammines in both structures, the differences are less than 2σ.

The hypoxanthine, the ruthenium, and the ammine nitrogen trans to the heterocyclic ligand all lie in a crystallographic mirror plane. While some bending about the C(4) to C(5) bond has been observed for some nonmetalated hypoxanthines,[18,24] the presence of such a mirror plane in these complexes requires planarity of the hypoxanthine ligand. Aside from the lack of bending in these complexes, the bond distances and angles for the coordinated hypoxanthine ligands reported here are essentially the same as those reported for hypoxanthine hydrochloride monohydrate.[25]

The two complexes exhibit different packing arrangements with the N(7) compound crystallizing in a lattice which contains three waters of solvation per complex ion. These water molecules form hydrogen bonds as follows: O(2) to N(9), 2.75 (2) Å; O(2) to Cl(2), 3.14 (1) Å; O(3) to N(3), 2.90 (1) Å; O(3) to Cl(3), 3.23 (1) Å. The coordination of $(NH_3)_5Ru^{III}$ to the N(7) position of hypoxanthine brings the purine oxygen into close proximity with two of the cis ammines. These ammines are symmetry related with the oxygen fitting between them to minimize repulsion and with a O(1) to N(10) distance of 2.88 (1) Å, which is within the range expected for hydrogen bonding.

While the hypoxanthine ligands are separated by a perpendicular distance of 3.41 Å, which is similar to the intermolecular stacking distances (3.25–3.41 Å) known for purine bases, there is very little overlap of the hypoxanthine ligands, in the N(7) compound, with only the C(2) to N(3) bond of two centrosymmetrically center-related molecules eclipsed. On the other hand, the N(9)-coordinated compound is more compact with no molecules of hydration. While the perpendicular distance separating the purines remains 3.41 Å, the degree of overlap is much greater.

(23) Krentzien, H. J.; Clarke, M. J.; Taube, H. *Bioinorg. Chem.* **1975**, *4*, 143–151 and references contained thereln.
(24) Sletten, J.; Jensen, L. H. *Acta Crystallogr.* **1969**, *B25*, 1608–1614.
(25) Clarke, M. J.; Taube, H. *J. Am. Chem. Soc.* **1974**, *96*, 5413.

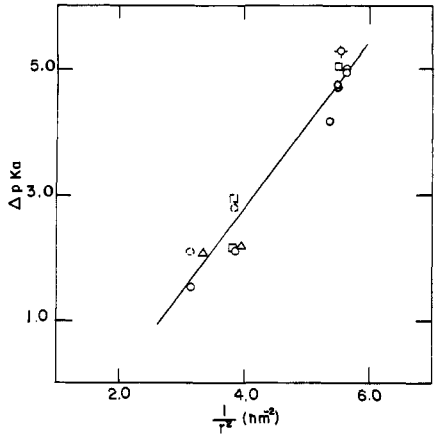

Figure 3. Plot of ΔpK_a vs. r^{-2} for a series of neutral and anionic ligand complexes of $(NH_3)_5Ru^{III}$. Circles are from ref 10, triangles from ref 11, and squares from ref 25, and star is from ref 27.

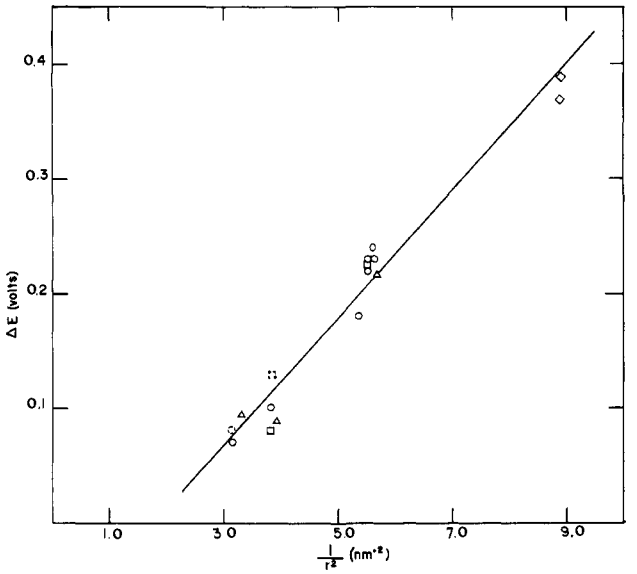

Figure 4. Plot of ΔE vs. r^{-2} for a series of neutral and anionic ligand complexes of $(NH_3)_5Ru^{III}$. References for data points are the same as in Figure 3. Diamonds are from ref 12.

The pyrimidine rings of center-related 7-methylhypoxanthine ligands overlay so that the carbonyl group of one nearly eclipses the N(3) of the other.

Free Energy Correlations. A plot of the increase in acidity of a similar series of heterocyclic ligands upon coordination to $(NH_3)_5Ru^{III}$ as a function of r^{-2}, where r is the distance between the metal and the ionization site, is given in Figure 3. The complexes employed are limited to those with neutral or anionic ligands having the same tautomeric form as the free ligand. Within these constraints and the given range of r ($4.2 < r < 5.6$ Å), the correlation is sufficiently good so as to be used for predictive purposes.

A similar correlation, but without the restriction of similar tautomeric forms for the free and complexed ligands, is illustrated in Figure 4 between r^{-2} and E, where ΔE is the difference in reduction potential for a complex and its conjugate base. This relationship extends over a somewhat larger range in r of ($3.4 < r < 5.6$ Å). Since both ΔpK_a and ΔE correlate with r^{-2}, they also correlate very well with each other.

Linkage Isomerization Kinetics. The isomerization of 3-(7-MeHyp)$(NH_3)_5Ru^{III}$ to yield 9-(7-MeHyp)$(NH_3)_5Ru^{III}$ between pH 2 and 7 follows the rate law

$$-\frac{d[N(3)]}{dt} = \frac{k_1[H^+] + k_0K_a}{[H^+] + K_a}[N(3)] = k_{obsd}[N(3)] \quad (1)$$

where [N(3)] is the total concentration of the N(3)-coordinated isomer, k_0 is the isomerization rate constant for the N(1) deprotonated form, k_1 is the rate constant for the neutral ligand complex, and K_a (1.51×10^{-5}) is the acidity constant for the neutral ligand complex.[10] A least-squares fit to the plot of k_{obsd} vs. pH as shown in Figure 5 yielded $k_0 = (2.2 \pm 1.7) \times 10^{-6}$ s^{-1} and $k_1 = (1.25 \pm 0.01) \times 10^{-4}$ s^{-1} at 37 °C and an ionic strength of 1.0. As indicated by the rate law, the values of k_{obsd} were independent of both the complex ion and chloride ion concentrations. All kinetic runs were observed to go essentially to completion. Activation parameters for k_1 were determined to be $\Delta H^{\ddagger} = 90 \pm 9$ kJ/mol and $\Delta S^{\ddagger} = -31 \pm 6$ J/(mol K).

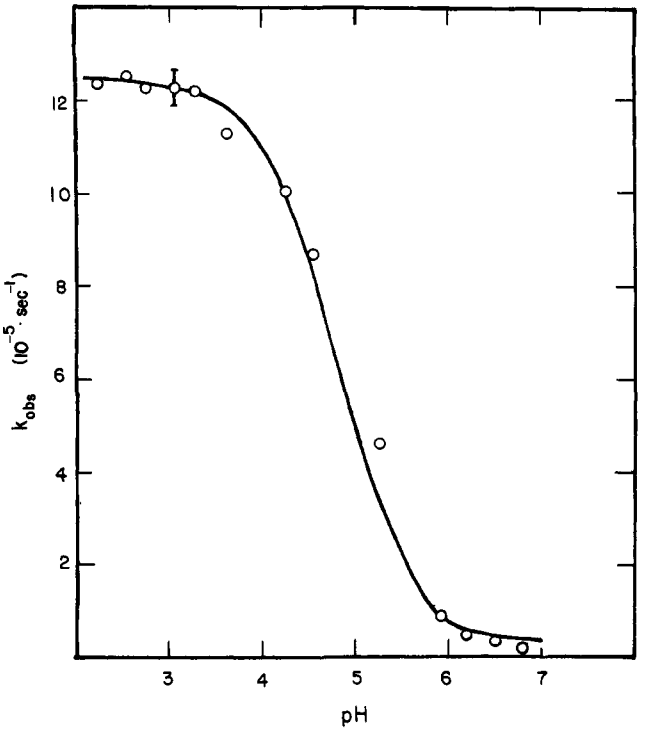

Figure 5. Plot of k_{obsd} vs. pH at 37 °C. Solid line was the calculated best fit by using eq 1, and the rate constants were reported in the text.

Above pH 5 isosbestic points were no longer observed over the entire course of the reaction. Monitoring these runs by HPLC revealed that a small portion (5% at pH 6.8) of the N(3) isomer was hydrolyzing to release the free ligand. Similar monitoring of solutions of the N(9) isomer under the same conditions yielded no indication of hydrolysis.

Discussion

Structure. The isolation of a single monomeric product in the formation of (dIno)$(NH_3)_5Ru^{III}$ and in its acid hydrolysis to yield exclusively 7-(Hyp)$(NH_3)_5Ru^{III}$ unequivocally establishes N(7) as the coordination site for $(NH_3)_5Ru^{III}$ on inosine and deoxyinosine.[10] Close analogies in spectra and chemical properties of the corresponding complexes with guanosine, deoxyguanosine, and 5′-guanosine monophosphate further establish N(7) as the binding site on these ligands as well.[10,25] Due to steric hindrance, alkylation, or protonation of the other nitrogen positions in these nucleosides or nucleotides at neutral pH, N(7) appears to be favored on both thermodynamic and kinetic grounds. However, when these other positions are not blocked, the metal coordinates in substantial amounts to all available imine nitrogens. Finally, similarities between the hypoxanthine compound reported here and the guanine complex isolated from the acid hydrolysis of $[(NH_3)_5Ru^{III}]_n$–DNA indicate that N(7) is also the kinetically preferred coordination site for amminеruthenium(III) ions on helical nucleic acids.[12,26]

In harmony with the greater thermodynamic affinity of $(NH_3)_5Ru^{III}$ for imidazole over ammonia,[27] Ru–N bond distance is

(26) Clarke, M. J.; Buchbinder, M.; Kelman, A. D. *Inorg. Chem. Acta* **1978**, *27*, L87–L88.

slightly shorter for coordination to the purine imidazole nitrogens than to the ammine nitrogens. In view of the relatively higher affinity of ammonia for protons and other hard Lewis acids it is probable that the imidazole portion of the purine can function as a more polarizable ligand toward Ru(III).[28] This may well occur through donation of electron density from the π system of the purine into the partially filled d_π orbital on the metal ion, as has been suggested in the case of Ru(III) coordinated to an amide nitrogen.[6]

Hydrogen bonding between proton donor ligands of a metal ion coordinated at N(7) and the exocyclic oxygen of hypoxanthine and guanine derivatives has been suggested as a factor contributing significantly to the stability of these complexes.[3] While this appears to be quite true for many first-row transition-metal complexes, it should be noted that the geometry of the ammines about the oxygen in 7-(Hyp)$(NH_3)_5Ru^{III}$ is sterically enforced by the coordination of the metal ion. Given the bending of the metal ion and the exocyclic oxygen away from each other and the nonlinear, bifurcated nature of these hydrogen bonds, it is doubtful that they add significantly to the net bonding interaction. However, the ability to form some type of hydrogen bond probably does serve to compensate for the steric repulsion between the cis ligands and the exocyclic oxygen.

While purines tend to stack both in crystalline form and in aqueous solution, any such stacking of cationic metallopurines must allow for steric and Coulombic repulsions between the metal centers. Therefore, strong stacking interactions are not evident in these crystal structures. However, a greater degree of overlap occurs between the pyrimidine rings of the N(9)-coordinated complex, since in this isomer the metal is distal from the carbonyl group and so allows this functionality to overlap with the pyrimidine ring of a second 7-MeHyp ligand.

Free Energy Correlations. The linear relationship of ΔpK_a with r^{-2} is similar to that encountered in the Kirkwood–Westheimer equation,[29] which has long been used to correlate substituent effects on organic acids[30]

$$\Delta pK_a = \frac{q\mu \cos\theta}{D_e r^2}$$

where q is the charge at the ionization site, μ is the dipole moment of the substituent, and D_e is the effective dielectric constant. This model assumes that field effects arising from ion–dipole interactions predominate in stabilizing the conjugate base. These same electrostatic interactions can be similarly expected to affect the free energy difference between the two ruthenium oxidations as a function of distance. The Kirkwood–Westheimer relationship also includes a directional term which is dependent on the angle θ between the substituent dipole and the vector **r**; however, since it is often difficult to determine the value of this term, most correlations of experimental data using this relation have held the angular dependency essentially constant.[31] In the case of a highly charged substituent it may be preferable to regard this portion of the molecule as the ion and the distribution of charges around the deprotonation site as a collection of dipoles,[32] which leads to further difficulty in fixing a single directional term. In the present case, attempts to correct for the directionality of the Ru(III)–L bond with respect to the proton ionization site yielded a significantly poorer straight-line fit of the thermodynamic data than a correlation with r^{-2} alone.

However good the correlation, explaining such behavior only in electrostatic terms would be overly simplistic, since effects transmitted through the σ and π frameworks should also play significant roles. Inductive and resonance effects no doubt account for the larger value of ΔpK_a when $(NH_3)_5Ru^{III}$ is coordinated to imidazole over the corresponding $(NH_3)_5Co^{III}$ complex.[33] Moreover, unreasonable values of either thermodynamic quantity result from linear extrapolations to very long values of **r**. Such plots must curve so as to lead to ΔpK_a and ΔE values of zero as r^{-2} also decreases to zero. Nevertheless, in the range of distances reported here, which encompasses most cases encountered with purine and pyrimidine ligands, the inverse square term dominates when other effects are held approximately constant by dealing with the same metal ion coordinated to similar sites. Such correlations can be of considerable utility in assigning linkage isomers and in developing methods to isolate new species involving these ambidentate ligands.

Isomerization Kinetics. Since the N(3) to N(9) linkage isomerization proceeds essentially to completion over the entire pH range investigated, the N(9) form must be substantially favored for coordination to $(NH_3)_5Ru^{III}$. This is understandable on the basis of relative electron densities at the two possible binding sites.[34] Preferred resonance forms place a lone pair at N(9) of the imidazole ring which should enhance both σ and π interactions with the metal ion. A decrease in the difference between the available electron densities at the two coordination sites, which is reflected in a 20-fold decrease in rate, occurs upon deprotonation of the N(1) site, since a net negative charge then resides on the pyrimidine ring. That the N(3) isomer can be formed in abundance is an artifact of the synthetic method which involves addition of the metal as Ru(II). In this oxidation state back-bonding becomes important and this is favored in the pyrimidine ring over the imidazole ring.[10,35,36]

The isomerization proceeds at a surprisingly rapid rate for both the neutral and anionic ligand forms. By way of comparison, the substitution of ammonia by chloride onto $(NH_3)_6Ru^{III}$ occurs with a half-life of 1.6 years.[37] In view of this, the steric arrangement of the entering and leaving nitrogens on the hypoxanthine ligand undoubtedly plays an important role. The N(9) atom is only 3.4 Å from the metal, so that the lone pair from this nitrogen impinges directly on an octahedral face of the Ru(III) and so facilitates the intramolecular isomerization. The intramolecularity of the reaction is confirmed by its strictly following first-order reaction kinetics and being independent of the counterion present. The negative entropy of activation is in the range expected for intramolecular linkage isomerizations[38] and is consistent with a loss of a rotational degree of freedom around the Ru–N(3) bond in the transition complex. Thus the existence of a N(3)–Ru–N(9)-bridged species is strongly implied in the transition state.[38]

While this particular type of isomerization is precluded in complexes with nucleosides and nucleic acids, these results taken in the context of other movements of pentaammineruthenium ions on similar ligands[11,12] have general implications for the interactions of substitution inert metal ions with nucleic acids.[6] It is quite possible that variations in the pH or redox environment around a metal ion can induce the metal to move between adjacent coordination sites on a nucleic acid at a rate much more rapid than that for dissociation from the polymer. This opens the possibility of the metal migrating to a site which would lead to a significantly greater (or lesser) probability of mutagenicity. Thus, the kinetically preferrred coordination site under the conditions holding during the initial attack of the metal ion need not be the one(s) directly resulting in the physiological response.

Acknowledgment. Preliminary investigations of the structures reported here were performed by M. Rose, T. D. Hayden, and A. Fried at Boston University. Initial studies of the isomerization kinetics were done by Mr. A. Maffei at Boston College. We are

(27) Sundberg, R. J.; Bryan, R. F.; Taylor, I. F.; Taube, H. *J. Am. Chem. Soc.* **1974**, *96*, 381.
(28) Purcell, K. F.; Kotz, J. C. "Inorganic Chemistry"; W. B. Saunders: Philadelphia, 1977; p 221.
(29) Kirkwood, J. G.; Westheimer, F. H. *J. Chem. Phys.* **1938**, *6*, 506–512.
(30) Ehrenson, S. *Prog. Phys. Org. Chem.* **1964**, *2*, 195.
(31) Wilcox, C. F.; Leung, C. *J. Am. Chem. Soc.* **1968**, *90*, 336–341.
(32) Constant, W. "Theoretical Physics"; Addison-Wesley: Reading, MA, 1958; pp 142–151.
(33) Brown, G. M.; Sutton, J. E.; Taube, H. *J. Am. Chem. Soc.* **1978**, *100*, 2767.
(34) Yu, C.; Peng, S.; Akiyama, I.; Lin, J.; LeBreton, P. R. *J. Am. Chem. Soc.*, **1978**, *100*, 2303–2307 and references therein.
(35) Kuehn, C.; Taube, H. *J. Am. Chem. Soc.* **1976**, *98*, 689.
(36) Shepherd, R. E.; Taube, H. *Inorg. Chem.* **1973**, *12*, 1392–1401.
(37) Armor, J. N. Ph.D. thesis, Stanford University, 1970.
(38) Reference 13, p 339.

also grateful to Dr. B. Gimarc (University of South Carolina) for a helpful discussion. This work was supported by PHS Grant GM 26390 from the National Institute of General Medical Sciences.

Supplementary Material Available: Tables of structure factor amplitudes for 7-[(Hyp)$(NH_3)_5$Ru]$Cl_3 \cdot 3H_2O$ and 9-[(7-MeHyp)$(NH_3)_5$Ru]Cl_3, of thermal parameters, of k_{obsd} as a function of pH, and of data for ΔpK_a and ΔE vs. r^{-2} free energy correlations, a plot of k_{obsd} vs. T^{-1}, and a plot of ΔpK_a vs. ΔE (37 pages). Ordering information is given on any current masthead page.

Trigonal-Bipyramidal Bis(neopentylidene), Neopentylidene/Ethylene, and Bis(ethylene) Complexes of Tantalum and How They React with Ethylene. A Catalyst for Rapidly Dimerizing Ethylene to 1-Butene

J. D. Fellmann, R. R. Schrock,* and G. A. Rupprecht

Contribution from the Department of Chemistry, 6-331, Massachusetts Institute of Technology, Cambridge, Massachusetts 02139. *Received January 29, 1981*

Abstract: We have prepared trigonal-bipyramidal bis(neopentylidene) complexes $[Ta(CHCMe_3)_2(R)L_2$, R = Cl, Me, Et, Bu, Np (Np = CH_2CMe_3), or mesityl, L = PMe_3], neopentylidene/ethylene complexes $[Ta(CHCMe_3)(C_2H_4)(R)L_2$, R = Et or Np], and bis(ethylene) complexes $[Ta(C_2H_4)_2(R)L_2$, R = Et or Np] by reactions involving abstraction of an α- or β-hydrogen atom from one alkyl group by another alkyl group. The PMe_3 ligands in these TBP molecules are found in the axial positions, the neopentylidene ligands lie in the trigonal plane, and the ethylene ligands line up along the L-Ta-L axis. Every complex which contains an ethyl or neopentyl ligand reacts with ethylene to give a catalyst which rapidly dimerizes ethylene to 1-butene. We propose that tantalacyclobutane complexes can form only when ethylene adds to the metal and that rearrangement of a TaC_3 ring by a β-hydride process is slow relative to the rate of opening a TaC_3 ring by migration of an α-hydrogen atom (from neopentyl) or a β-hydrogen atom (from ethyl or neoheptyl) to C_α of the ring. The final product of these reactions is postulated to be $Ta(C_2H_4)_2(Bu)L_2$. The butyl ring forms in the last step when a β-hydrogen atom from another ligand transfers to C_α of a tantalacyclopentane ring. We believe ethylene is dimerized by $Ta(C_2H_4)_2(Bu)L_2$ via a related "tantalacyclopentane" mechanism and not by a mechanism which involves insertion of ethylene into a tantalum-ethyl bond. Some variation of this "metallacyclopentane mechanism" for dimerizing ethylene is a valid, mechanistically indistinguishable alternative to the "insertion mechanism" which has dominated proposals in the literature to date.

Some time ago we found that $Ta(CHCMe_3)Np_3$ (Np = CH_2CMe_3) in the presence of at least 2 equiv of PMe_3 in pentane at 25 °C will dimerize ethylene rapidly and selectively to 1-butene. Since such selectivity is rare,[1] we set out to learn more about this reaction. In the process we discovered trigonal-bipyramidal (TBP) complexes which contain two neopentylidene ligands,[2] one neopentylidene and one ethylene ligand, and two ethylene ligands. Some of these complexes react rapidly with ethylene to give the dimerization catalysts.[3] Others give catalytically inactive products. Since we can identify the predominant species in a catalyst solution, we can propose a mechanism for dimerizing ethylene to 1-butene. Our proposal differs significantly from the usual one in that the C-C bond is postulated to form via a metallacyclopentane complex and not by insertion of ethylene into a metal-ethyl bond. This paper reports the full details of this work.

Results

Bis(neopentylidene) Complexes. $TaNp_4Cl$ decomposes at ca. 0 °C to give transient $Ta(CHCMe_3)Np_2Cl$.[4] In the presence of PMe_3, another equivalent of neopentane is formed and yellow $Ta(CHCMe_3)_2(Cl)L_2$ (L = PMe_3) can be isolated in high yield (eq 1). $Ta(CHCMe_3)_2(Cl)L_2$ also can be prepared (but in lower

$$TaNp_4Cl \xrightarrow{-CMe_4} \text{“}Ta(CHCMe_3)Np_2Cl\text{”} \xrightarrow[2PMe_3]{-CMe_4} Ta(CHCMe_3)_2(Cl)(PMe_3)_2 \quad (1)$$

yield) as shown in eq 2. $Ta(CHCMe_3)_2(Cl)L_2$ is moderately soluble in pentane, can be sublimed (with some decomposition), is a monomer in cyclohexane, and shows a parent ion peak in its mass spectrum.

$$Ta(CHCMe_3)Cl_3L_2^{5} + MgNp_2(\text{dioxane}) \xrightarrow[\text{ether}]{-30\ ^\circ C} Ta(CHCMe_3)_2(Cl)L_2 \quad (2)$$

$Ta(CHCMe_3)_2(Cl)L_2$ reacts with lithium alkyls to give the derivatives shown in eq 3 in high yield. $Ta(CHCMe_3)_2(Np)L_2$

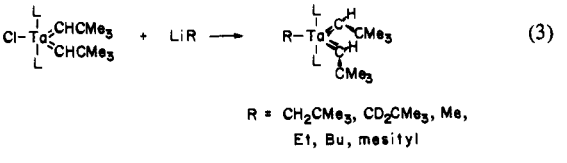

(3)

R = CH_2CMe_3, CD_2CMe_3, Me, Et, Bu, mesityl

also can be prepared directly from $Ta(CHCMe_3)Np_3$ by addition of PMe_3 (eq 4).

$$Ta(CHCMe_3)Np_3 + 2L \xrightarrow{-CMe_4} Ta(CHCMe_3)_2(Np)L_2 \quad (4)$$

(1) Lefebvre, G.; Chauvin, Y. In "Aspects of Homogeneous Catalysis"; R. Ugo, Ed.; Carlo Manfredi: Editore-Milano, 1970; Vol. 1, pp 107-201, and references therein.
(2) Fellmann, J. D.; Rupprecht, G. A.; Wood, C. D.; Schrock, R. R. *J. Am. Chem. Soc.* **1978**, *100*, 5964-5966.
(3) Fellmann, J. D.; Rupprecht, G. A.; Schrock, R. R. *J. Am. Chem. Soc.* **1979**, *101*, 5099-5101.
(4) Schrock, R. R.; Fellmann, J. D. *J. Am. Chem. Soc.* **1978**, *100*, 3359-3370.
(5) Rupprecht, G. A.; Messerle, L. W.; Fellmann, J. D.; Schrock, R. R. *J. Am. Chem. Soc.* **1980**, *102*, 6236-6244.

0002-7863/81/1503-5752$01.25/0